

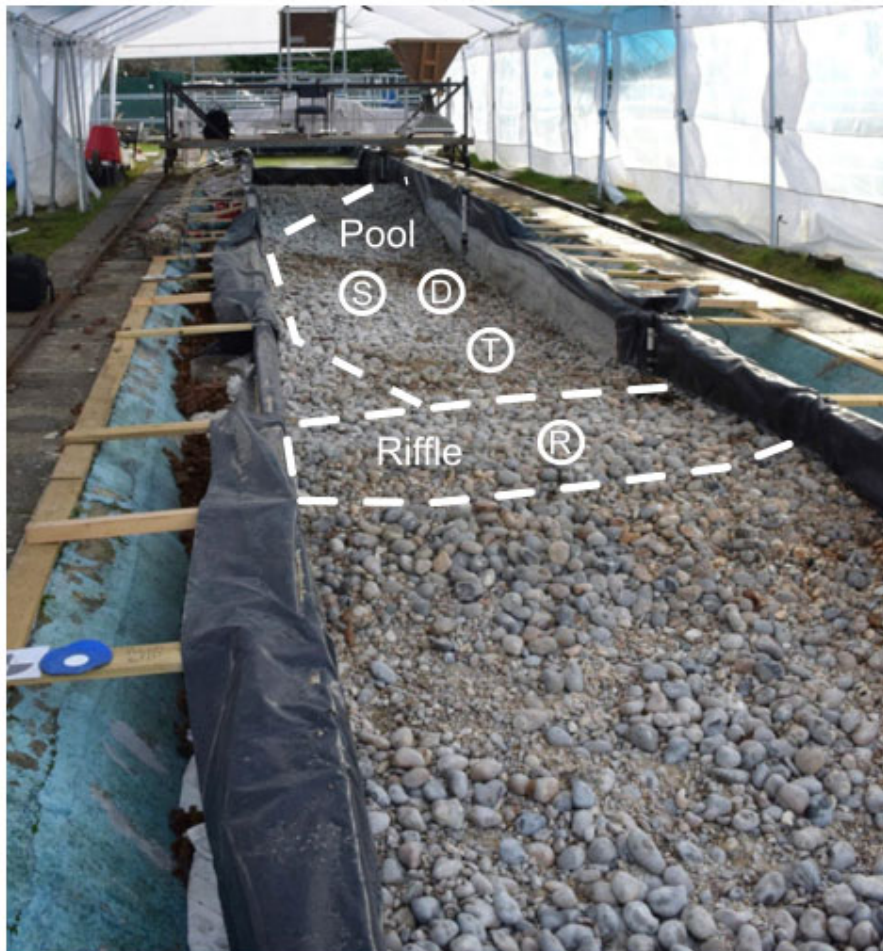
1 **Data Repository 1: X-ray computed tomography reveals that grain protrusion controls critical**
2 **entrainment shear stress in fluvial gravels**

3 Rebecca Hodge, Hal Voepel, Julian Leyland, David Sear, Sharif Ahmed

4

5 **Section 1: Flume Morphology**

6 The morphology of the flume bed is shown in Fig. DR1.



7

8 Figure DR1: Flume set up, showing the riffle-pool topography. Flow is from top to bottom of the image. Circles
9 show the approximate locations of the baskets in the riffle (R), pool tail (T), deep pool (D), and shallow pool (S).
10 Flume dimensions are 60 x 2.1 x 0.7 m.

11

12

13

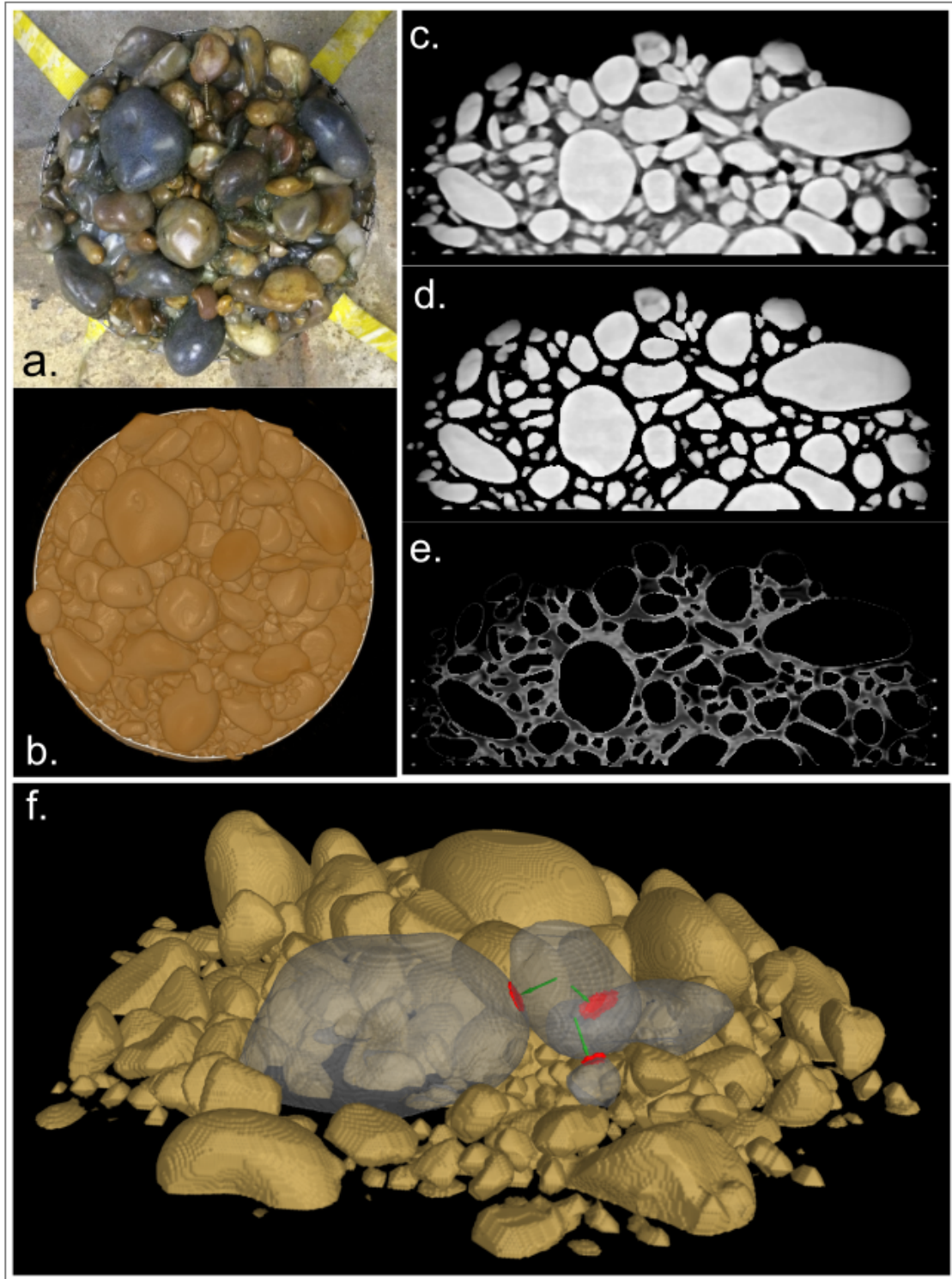
14

15

16

17

18 **Section 2: X-ray computed tomography (XCT) images of the baskets**
19 Images of different stages of the XCT processing methods are shown in Fig. DR2.



20
21 Figure DR2: a and b) photo and scan of basket surface; c to e) cross-sections through XCT scan showing entire
22 basket, grains only and matrix only respectively. The different components were segmented using a semi-
23 automated classification; f) 3D image of a set of grains, with a surface grain and three supporting grains shown

24 as translucent. For these four grains grain-grain contacts (red patches) and particle-to-contact vectors (green)
25 are shown.

26

27 **Section 3: Methods for comparison with bedload models:**

28 We use the XCT results to calculate the number of grains that would be entrained at different values
29 of τ^* , and compare these numbers to the number of grains that are predicted to be entrained using
30 both the Meyer-Peter Muller (1948) and Wilcock and Crowe (2003) bedload transport models.

31 For the XCT data, we assume that the total area, A , of all 20 baskets is arranged as a single area with
32 downstream length, L , which is a grain step length, and width $w = A/L$. Values of τ_c for each grain are
33 converted to $\tau_{c,g}^*$ using the D_{50} for all baskets (23 mm). For each applied τ^* , all grains with $\tau_{c,g}^* < \tau^*$
34 will leave A in a time step with duration t .

35 One approach to calculating t is to use grain saltation velocity (v): $t = v/L$, which gives the time for all
36 grains to leave area A . However, this assumes that grains are instantaneously entrained and move at
37 velocity v . However, their actual velocity will be a virtual velocity that incorporates rest periods and
38 so is a fraction of v . We therefore add a transport rate reduction factor (F) such that $t = Fv/L$; when F
39 = 1, grains are travelling at their saltation velocity with no rest periods.

40 For the bedload transport model we use both Meyer-Peter and Muller (1948) and Wilcock and
41 Crowe (2003), which give bedload transport rates (q_s) in $\text{m}^3 \text{m}^{-1} \text{s}^{-1}$. These are converted to number of
42 grains using V , the volume of a spherical D_{50} grain. For both bedload models we use a uniform grain
43 size of D_{50} . Although we could implement Wilcock and Crowe (2003) with a full grain size
44 distribution, the uncertainties around other components of this comparison mean that this level of
45 sophistication is unnecessary. Furthermore, our data suggest that τ_c is not a significant function of
46 grain size (Fig. 2L). To compare the model bedload transport rates to the XCT scan results, we
47 calculate the number of grains (N) as $N = (q_s w t)/V$, which is equal to $N = (q_s (A F v/L))/V$.

48 Implementing this calculation requires estimates of v , L , F and $\tau_{c,m}^*$, where the latter is the critical
49 shear stress implemented in the bedload models. For v and L we use equations fitted by Sklar and
50 Dietrich (2004) to a selection of data from saltating grains in which v and L are power functions of
51 $[(\tau^*/\tau_{c,m}^*) - 1]$, with exponents of 0.56 and 0.88 respectively. We also require a value of F . Schmidt
52 and Ergenzinger (1992) report mean step lengths and rest periods for radio-tracked particles of 19 m
53 and 1380 s respectively, with travel velocities between 0.01 and 0.5 m s^{-1} giving $F = 0.02$ to 0.6.
54 Habersack (2001) shows for a radio-tracked particle in a small flood $F = 0.03$, whereas in larger event
55 $F = 0.25$. To account for the uncertainty in both $\tau_{c,m}^*$ and F , we calculate relationships between τ^*
56 and N for both bedload models using $\tau_{c,m}^*$ ranging from 0.03 to 0.06, and F from 0.02 to 0.2. The up-
57 kick at small values of τ^* for the Wilcock and Crowe (2003) model is because as τ^* decreases, the
58 timestep increases faster than the decrease in the bedload transport rate.

59 **References**

60 Habersack, H. M. (2001), Radio-tracking gravel particles in a large braided river in New Zealand: a
61 field test of the stochastic theory of bed load transport proposed by Einstein. *Hydrol. Process.*, 15:
62 377–391. doi:10.1002/hyp.147

63 Schmidt, K.-H. and Ergenzinger, P. (1992), Bedload entrainment, travel lengths, step lengths, rest
64 periods—studied with passive (iron, magnetic) and active (radio) tracer techniques. *Earth Surf.*
65 *Process. Landforms*, 17: 147–165. doi:10.1002/esp.3290170204

66 Sklar, L.S., Dietrich, W.E., 2004. A mechanistic model for river incision into bedrock by saltating bed
67 load. Water Resour. Res. 40, W06301. doi:10.1029/2003WR002496

Supplementary Table

2020044_Table DR1.xlsx